

# PDGF2/*c-sis* mRNA Leader Contains a Differentiation-linked Internal Ribosomal Entry Site (D-IRES)\*

(Received for publication, November 15, 1996)

Jeanne Bernstein‡, Osnat Sella‡, Shu-Yun Le§, and Orna Elroy-Stein‡¶

From the ‡Department of Cell Research and Immunology, George S. Wise Faculty of Life Sciences, Tel Aviv University, Tel Aviv 69978, Israel and the §Laboratory of Mathematical Biology, DCBDC, NCI, NIH, Frederick, Maryland 21702

**It has become clear that a given cell type can qualitatively and quantitatively affect the expression of the platelet-derived growth factor B (PDGF2/*c-sis*) gene at multiple levels. In a previous report, we showed that PDGF2/*c-sis* 5'-untranslated region has a translational modulating activity during megakaryocytic differentiation of K562 cells. This study points to the mechanism used for this translational modulation. The unusual mRNA leader, which imposes a major barrier to conventional ribosomal scanning, was found to contain an internal ribosomal entry site that becomes more potent in differentiating cells and was termed differentiation-linked internal ribosomal entry site (D-IRES). The D-IRES element defines a functional role for the cumbersome 1022-nucleotide-long mRNA leader and accounts for its uncommon, evolutionary conserved architecture. The differentiation-linked enhancement of internal translation, which provides an additional step to the fine tuning of PDGF2/*c-sis* gene expression, might be employed by numerous critical regulatory genes with unusual mRNA leaders and might have widespread implications for cellular growth and development.**

The mechanisms that control the expression of genes operate at a variety of levels that include all the transcriptional and post-transcriptional stages. In a rapidly growing number of examples, gene expression is regulated also at the level of translation, usually involving the translational initiation step. mRNA leaders that mediate efficient translation initiation are short (50–70 nt),<sup>1</sup> contain 5'-m<sup>7</sup>G cap structure, and lack stable secondary structures as well as upstream AUG codons (reviewed in Ref. 1). Interestingly, genes encoding for regulatory proteins involved in growth and development often do not meet these criteria and produce long, structured, and upstream AUG-burdened mRNA leaders. These features are incompatible with efficient translation by the ribosomal scanning mech-

anism which is considered valid for the translation of the vast majority of cellular and viral mRNAs (2).

Platelet-derived growth factor (PDGF) is a potent mitogen of all cells of mesenchymal origin and has a major role in wound healing as well as in embryogenesis and development. PDGF consists of homo- or heterodimers of two protein chains, PDGF-A and PDGF-B. The PDGF-B chain is the product of the PDGF2/*c-sis* proto-oncogene, which has a neoplastic transformation potential and is expressed in various types of tumor tissues. Normally, the expression of PDGF2/*c-sis* is tightly regulated due to multiple control mechanisms at the transcriptional and post-transcriptional levels. PDGF2/*c-sis* mRNA has a striking architecture: it has a 723-nt coding region and exceptionally long 5'- and 3'-untranslated regions (UTRs) of 1022 and 1625 nt, respectively. The extraordinarily long 5'-UTR contains stable secondary structures and three mini-open reading frames upstream of the translation initiator AUG codon. As such, it imposes a significant barrier to the linear ribosomal scanning from the 5'-m<sup>7</sup>G cap structure toward the fourth AUG codon, thereby serving as a potent translational inhibitor (reviewed in Ref. 3).

One of the major sites of PDGF synthesis is within bone marrow megakaryocytes, the platelets progenitor cells. As shown in our earlier work, the 5'-UTR-mediated translational inhibition was relieved at a certain time window during megakaryocytic differentiation (4). The translation inhibitory effect of PDGF2/*c-sis* 5'-UTR was not relieved by elevated levels of the cap-binding protein eIF4E (4), nor by mutations of the upstream AUG codons (5, 6). These observations prompted us to examine whether during the differentiation process PDGF2/*c-sis* mRNA is translated by an alternative cap-independent initiation mechanism.

A cap-independent mechanism for translation initiation has been demonstrated for picornaviruses, which lack 5'-m<sup>7</sup>G cap and have long, structured, AUG-burdened mRNA leaders. An internal ribosomal entry site (IRES) was found in members of the cardio-, aphtho-, entero-, rhino-, and hepatoviruses, as well as in pestiviruses. Although there is no similarity in the primary sequences of the different IRES elements, there are similarities in their secondary structural features (reviewed in Refs. 7 and 8). Interestingly, internal translation has been found also for the cellular genes of mammalian Bip (9), FGF2 (10), IGF-II (11), eIF4G (12), and *Antennapedia* of *Drosophila melanogaster* (13). In this study we demonstrate that the PDGF2/*c-sis* 5'-UTR contains an IRES element that responds to changes in the cellular milieu and facilitates translation of the mRNA during megakaryocytic differentiation. Computer analysis involving inspection of compensatory base changes among divergent PDGF2/*c-sis* sequences from human, cat, and mouse predicts structural features within the 5'-UTR that are common to known IRES elements.

This study provides the first example for a differentiation-

\* This work was supported by the Charles H. Revson Foundation administered by the Israel Science Foundation and in part by Grant 2918 from the Chief Scientist's Office of Ministry of Health, Israel (to O. E. S.). The costs of publication of this article were defrayed in part by the payment of page charges. This article must therefore be hereby marked "advertisement" in accordance with 18 U.S.C. Section 1734 solely to indicate this fact.

The nucleotide sequence(s) reported in this paper has been submitted to the GenBank™/EBI Data Bank with accession number(s) M19719

¶ To whom correspondence should be addressed. Tel.: 972-3-640-9153; Fax: 972-3-642-2046; E-mail: ORNAES@ccsg.tau.ac.il.

<sup>1</sup> The abbreviation used are: nt, nucleotide(s); PDGF, platelet-derived growth factor; 5'-UTR, 5' untranslated region; IRES, internal ribosomal entry site; D-IRES, differentiation-linked IRES; TPA, 12-*O*-tetradecanoylphorbol-13-acetate; bp, base pair(s); CAT, chloramphenicol acetyltransferase; LUC, luciferase; GAPDH, glyceraldehyde-3-phosphate dehydrogenase; CMV, cytomegalovirus; EMCV, encephalomyocarditis virus; HAV, hepatitis A virus; kb, kilobase pair(s).

linked IRES (D-IRES) element, which might be one of many inducible IRES elements in extraordinary mRNA leaders of cellular genes encoding critical regulatory proteins.

## EXPERIMENTAL PROCEDURES

### Plasmid Constructions

pT7CAT-LUC obtained from Dr. Sarnow (9) was digested with *Sall*, filled in, and ligated with 1-kb *NcoI-MluI* filled in fragment of pPD1 (4), to create pT7CPL. pT7CEL was constructed by three-part ligation of the following fragments: (i) 0.3-kb *Sall*(filled-in)-*NcoI* fragment from pT7CAT-LUC, (ii) 0.5-kb *ApaI*(filled-in)-*NcoI* fragment of pEMCV-CAT (14), and (iii) the backbone *NcoI* fragment of pT7CAT-LUC. To construct pT7CHL, 0.7-kb *Sall* fragment was generated from pHAV7 template (15) by polymerase chain reaction using oligonucleotide primers 5'-GGGGGTGACCTCACCGCGT-3' and 5'-GGGGGTGACCTAAATGCCCC-3', followed by *Sall* digestion and ligation into the *Sall* site of pT7CAT-LUC. The bi-cistronic plasmids under the CMV promoter were generated using pBI-FC1 or pHP-FC1 from Dr. A.-C. Prats as backbones (10). The following cloning steps were performed: 1.8-kb *NotI-SacI* fragment harboring the LUC gene was generated by polymerase chain reaction using pT7CAT-LUC (9) as template and oligonucleotide primers 5'-GGGGTTCGACGCGCCGCCCATGGAA-GACGCCAAAAACATA-3' and 5'-CCCCGAGCTCCATTCATCAATTGTC-3' and was inserted into *NotI* and *SacI* sites of pBluescript II SK+ (Stratagene) downstream of the T7 promoter to create pBS-LUC. In addition, the 1.8-kb *SacI-NotI* fragment harboring the LUC gene was ligated with the 4.1-kb *SacI-NotI* fragment of pBI-FC1 to create the bi-cistronic pCL plasmid. Intact or truncated *c-sis* 5'-UTRs were inserted into pBS-LUC plasmid, upstream to LUC. This was done by ligating pBS-LUC *SpeI-NcoI* fragment with polymerase chain reaction fragments which were generated by using pSis4.0 (5) as template and oligonucleotide primers homologous to specific *c-sis* 5'-UTR sequences. The following oligonucleotides, which bear synthetic *SpeI* or *NcoI* sites, were used: 5'-CCCCACTAGTGGCAACTTCTCTCC-3' (JB7) and 5'-CCCCCATGGCGACTCCGGGCGCCGCC-3' (OS35) to amplify the intact 5'-UTR (1-1022); 5'-CCCCACTAGTAACCGGAGCAGCCG-CAGC-3' (OS64) and 5'-CCAACCATGGCTTTGCAACGGCAGC-3' (OS65) to amplify region 215-488; and 5'-GGGTACTAGTGCTGCCGTGTC-3' (OS66) and 5'-CTCACCCCATGGCCCGGC-3' (OS67) to amplify region 475-870. The ATG of the *NcoI* site was designed to match exactly with the ATG of LUC. The *SpeI-SacI* fragment containing the full-length 5'-UTR fused to LUC was ligated with the 4.1-kb *SpeI-SacI* fragment of pBI-FC1 or pHP-FC1 to create pCPL or pHCPL, respectively. The *SpeI-SacI* fragments containing the truncated 5'-UTR fused to LUC were ligated with the 4.1-kb *SpeI-SacI* fragment of pSCT Bi28 to create pC(215-488)L and pC(475-870)L.

### Megakaryocytic Differentiation and Plasmid Expression

**Infection-Transfection**—Megakaryocytic differentiation was induced by treatment of exponentially growing K562 cells with TPA (Sigma) at concentration of 5 nM for 48 h. Infection-transfection was carried out in a six-well dish using  $10^6$  cells and 5  $\mu$ g of supercoiled plasmid DNA/well. 30 min prior to transfection, control or TPA-treated cells were infected with recombinant vaccinia virus vTF7-3 at multiplicity of infection of 1 plaque-forming unit/cell, followed by liposome-mediated transfection, as described previously (4).

**Electroporation**—100  $\mu$ g of supercoiled plasmid DNA per a total of  $10^7$  exponentially growing K562 cells resuspended in 0.8 ml of RPMI 1640 without serum were used for each electroporation pool, using an electric pulse of 240 V, 1500 microfarads (Easy Ject<sup>+</sup> electroporator, Equibio). Immediately following the electric pulse, the cells were transferred to RPMI 1640 medium supplemented with 50 units/ml of penicillin, 50  $\mu$ g/ml of streptomycin, and 15% fetal calf serum. 24 h after electroporation the cells were diluted to a final concentration of  $5 \times 10^5$  living cells (as determined by using trypan blue for counting) in RPMI 1640 supplemented with 10% fetal calf serum, with or without 5 nM TPA (Sigma), for 48 h.

**CAT and Luciferase Assays**—The TPA-treated and control transfected cells were harvested simultaneously for CAT and luciferase assays, as well as for RNA analysis. For the enzymatic activity assays, the cell pellet was lysed by three freeze-thaw cycles in 0.1 M Tris, pH = 8.0. CAT activity in the cells lysates was determined by a phase extraction assay, which quantified butyrylated <sup>3</sup>H-labeled chloramphenicol products by liquid scintillation counting, followed by xylene extraction (pCAT reporter gene system, Promega). LUC activity in the cell lysate was determined using TD-20e-Luminometer (Turner) following 15-s incubation of 1-5  $\mu$ g of the protein extract with 470  $\mu$ M luciferin (Sigma)

and 270  $\mu$ M coenzyme A (Sigma) in 20 mM K-Hepes, pH = 7.8, 1 mM EDTA, 4 mM MgAc, 1 mg/ml bovine serum albumin, and 530  $\mu$ M ATP. Total protein concentration in each sample was determined by the Bradford assay (16).

**RNA Analysis**—Total RNA was isolated from  $2 \times 10^7$  cells using Tri Reagent procedure (Tri Reagent®, MRC, Inc.), which is based on the phenol and guanidine thiocyanate in a monophasic solution. Poly(A)<sup>+</sup> RNA was purified from 150  $\mu$ g of total RNA using oligo(dT) magnetic beads (Dynabeads, Inc.). Poly(A)<sup>+</sup> RNA was subjected to Northern blot analysis according to standard procedures (17), using <sup>32</sup>P-labeled cDNA probes specific for the *CAT*, *PDGF2/c-sis*, *LUC*, or glyceraldehyde-3-phosphate dehydrogenase (*GAPDH*) genes. To quantify the RNA, the intensities of specific bands were determined using the phosphorimager (Fujix Bas 100, Fuji).

## RESULTS

**Effect of Megakaryocytic Differentiation on Activity of IRES Elements**—The leader of *PDGF2/c-sis* mRNA is highly complex and imposes a major difficulty to linear ribosomal scanning. However, as demonstrated previously, megakaryocytic differentiation of K562 cells alleviates its translational inhibitory effect (4). We therefore wished to examine whether *PDGF2/c-sis* mRNA leader harbors a weak IRES element which is activated upon differentiation. Since internal translation activity is known to be dependent on *trans*-acting factors (reviewed in Refs. 7 and 18), the performance of IRES elements is assumed to be affected by the cellular availability of such factors. Hence, the first objective was to determine whether the cellular environment created by the TPA-induced differentiation is more supportive for internal translation. Internal ribosomal entry is traditionally demonstrated using bi-cistronic expression plasmids. In these plasmids, the second cistron is not translated unless it is located immediately downstream to an active IRES which is downstream to the stop codon of the first cistron. Chloramphenicol acetyltransferase (*CAT*) and luciferase (*LUC*) reporter genes were used as the first or second cistrons, respectively, under control of the T7 promoter. The well characterized IRES elements of encephalomyocarditis virus (EMCV) or hepatitis A virus (HAV) were inserted between the two cistrons, downstream to the *CAT* translational stop codon, to create plasmids pT7CEL or pT7CHL, respectively. In addition, the 5'-UTR of *PDGF2/c-sis* was inserted between the two cistrons to create pT7CPL. Plasmid pT7CL, in which *LUC* is located immediately downstream to the stop codon of *CAT* (Fig. 1A), served as the control plasmid. The hybrid T7/vaccinia expression system was employed to express bi-cistronic mRNA from T7 promoter in the cytoplasm of control or TPA-treated K562 cells.

Control or TPA-treated K562 cells were infected with vTF7-3, a recombinant vaccinia virus that expresses the T7 RNA polymerase in the cytoplasm, and transfected with one of the above bi-cistronic plasmids. 24 h after the infection-transfection experiment, *CAT* and *LUC* enzymatic activities were measured. Fig. 1B illustrates the *LUC/CAT* ratio obtained in the differentiated cells relative to the control cells for each of the plasmids. As shown, the differentiation process generated a cellular milieu that facilitated the internal translation conferred by the viral IRES elements. The enhancement of EMCV IRES activity was about 3-fold whereas that of HAV was less prominent (Fig. 1B). Interestingly, differentiation-linked activation of the second cistron translation was also observed upon insertion of *PDGF2/c-sis* 5'-UTR (Fig. 1B, pT7CPL). This phenomenon led us to speculate that the mRNA leader of *PDGF2/c-sis* might contain an IRES element that gains activity upon certain cellular changes.

**Computerized Prediction of *c-sis* 5'-UTR mRNA Folding**—From studies on picornaviruses, IRES elements are known to have structural features that are important for their role as mediators of internal ribosomal entry (7, 18). The RNA structural analysis of *PDGF2/c-sis* 5'-UTR was performed by theo-

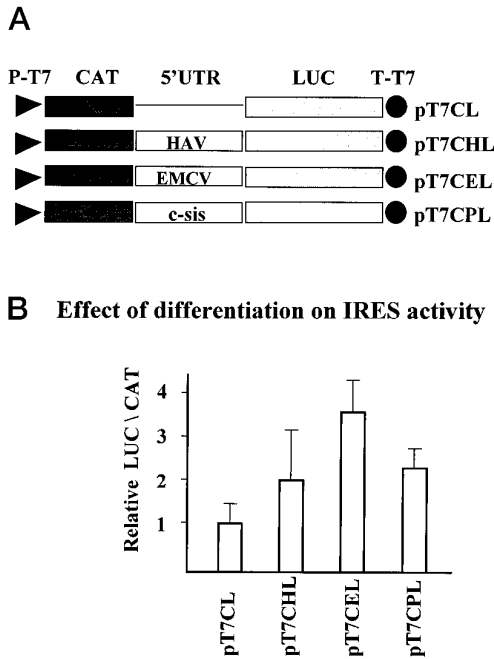


**FIG. 1. Effect of differentiation on activity of IRES elements.** A, schematic drawing of the T7 transcription unit of pT7CL, pT7CHL, pT7CEL, and pT7CPL plasmids. Triangles, T7 promoter (P-T7); dark boxes, the CAT coding sequence; open boxes, 5'-UTR of HAV, EMCV, or *c-sis* as indicated; light boxes, the LUC coding sequence; circles, T7 terminator (T-T7). B, control or TPA-treated cells were infected with  $\nu$ TF7-3 and transfected with each of the indicated plasmids (see "Experimental Procedures"). 24 h later, CAT and LUC enzymatic activities were determined. The data represent the LUC/CAT ratio obtained in the TPA-treated cells relative to control cells. The bars represent the average  $\pm$  S.E. of three independent transfection experiments.

retical prediction of RNA folding and phylogenetic analysis. In the structural analysis, the thermodynamically favored helical stems folded in the 5'-UTR were predicted by EFOLD, a method that computes all possible alternative RNA structures based on the fluctuation of thermodynamic energy parameters within the range of experimental errors for these parameters (19). These computed helical stems were evaluated by a statistical simulation SEGFOLD (20, 21) and verified by inspecting their conservation of complementarity and compensatory base changes among divergent PDGF sequences from human, cat, and mouse. Based on both the conserved and thermodynamic favored helical stems within these divergent 5'-UTR sequences, the possible RNA secondary structure was constructed. As shown in Fig. 2A, the predicted common RNA secondary structure is divided into six domains, A–F. Domain B, composed of the sequence from 191–685, was predicted to be an extensive RNA secondary structure of sufficient stability to inhibit the ribosome scanning process. Distinct Y-type stem-loop structures were observed just upstream of the first, third and fourth AUG codons. These conserved Y-type structures, denoted B5, D, and F (Fig. 2A), have significance scores of  $-1.75$ ,  $-1.87$ , and  $-2.57$ , respectively. Such significance scores suggest structural role for these regions (19). Structure B5 (512–581) is just 1 nt upstream of the first AUG triplet. Structures D (784–860) is just 9 nt upstream of the third AUG triplet, and structure F (934–1005) is about 17 nt upstream of the fourth AUG triplet. Structures D and F are composed of GC-rich sequences (more than 84% GC). Polypyrimidine sequences rich in U residues, that have been found to be important for viral IRES activity (22), are located in the Y-type structure B5 and in the stem-loop structure designated as B8 (Fig. 2B).

Two pseudoknot structures, denoted by the letter K in Fig. 2,

were predicted. One (K1) is formed by interaction between sequences in loop B5b of Y-type structure B5 with sequences in the loop of structure B7. The potential pseudoknot is present in the human, mouse, and cat structures, although the interacting sequences are not phylogenetically conserved. The second pseudoknot (K2) is formed by interaction of CCCG in the Y-type structure F loop (F1', Fig. 2B), with CGGG just downstream of it. The evolutionary conservation of this interaction suggests that the structure has a functional relevance.

A sequence complementary to the conserved 3'-end of 18 S rRNA was found at the 3'-end of the 5'-UTR, just upstream of the fourth AUG codon, from which the PDGF2/*c-sis* open reading frame begins. The region of complementarity was predicted to be single-stranded (G, Fig. 2, A and B). It is noteworthy that picornavirus IRES elements share a conserved complementary sequence to the 3'-end of human 18 S rRNA (23, 24).

All the above features are compatible with the notion that *cis*-elements within the 5'-UTR of PDGF2/*c-sis* confer internal translation initiation. A Y-type structure, followed by a pseudoknot interaction and a sequence complementary to 18 S rRNA, immediately upstream to the start codon of the internal translation, is a common structural feature observed in all IRES elements of picornaviruses, hepatitis C virus, and pestiviruses RNAs (23–25). All the Y-type structures predicted for human PDGF2/*c-sis* mRNA leader were found to be conserved in the feline and murine PDGF2 mRNA leaders. The evolutionary conservation of these distinct structures suggests a role in the IRES-dependent translation.

**Effect of Differentiation on Internal Translation Conferred by Truncated mRNA Leader**—The relevance of the results shown in Fig. 1B to a cellular setup in which transcription takes place in the nucleus was verified by determining the behavior of the bi-cistronic mRNA in the absence of vaccinia virus infection. To that end, another set of bi-cistronic plasmids was constructed employing the CMV promoter (Fig. 3A). In pCL plasmid, the LUC reporter gene was located immediately downstream to the translational stop codon of CAT, whereas in pCPL the entire PDGF2/*c-sis* 5'-UTR was located between the two cistrons. To determine the ability of specific structural motifs to mediate the TPA-linked IRES activity, two additional plasmids, pC(215–488)L and pC(475–870)L, were constructed according to the structural model of the 5'-UTR presented in Fig. 2A. In these plasmids, the regions spanning nucleotides 215–488 or 475–870 of the 5'-UTR were located between the two cistrons, respectively. Each of these plasmids was introduced into K562 cells by electroporation, followed by incubation of the cells in medium with or without TPA for 48 h. Following TPA treatment, CAT and LUC enzymatic activities and mRNA levels were detected. The integrity of the bi-cistronic mRNA was verified by Northern blot analysis using  $^{32}$ P-labeled cDNA probes specific for the CAT, LUC, or GAPDH genes. The endogenous GAPDH mRNA level served as internal control to monitor the plasmid-derived mRNA level present in each of the different samples. As observed in Fig. 3B, the expected 3.8-kb bi-cistronic mRNA was detected by both CAT and LUC probes. The anticipated reductions in the bi-cistronic mRNAs length were observed, as expected, from plasmids that contained the truncated 5'-UTR. An additional, unexpected, smaller mRNA picked up by the CAT probe probably reflects cross-hybridization with cellular mRNA, as seen previously by others (9). However, the LUC probe picked exclusively the bi-cistronic mRNA, indicating its integrity. Longer exposure of the blot after its hybridization with  $^{32}$ P-labeled LUC cDNA clearly demonstrated the absence of smaller LUC mRNA molecules (Fig. 3B), implying that LUC protein synthesis results from translation of the second cistron. Unexpectedly, TPA treatment

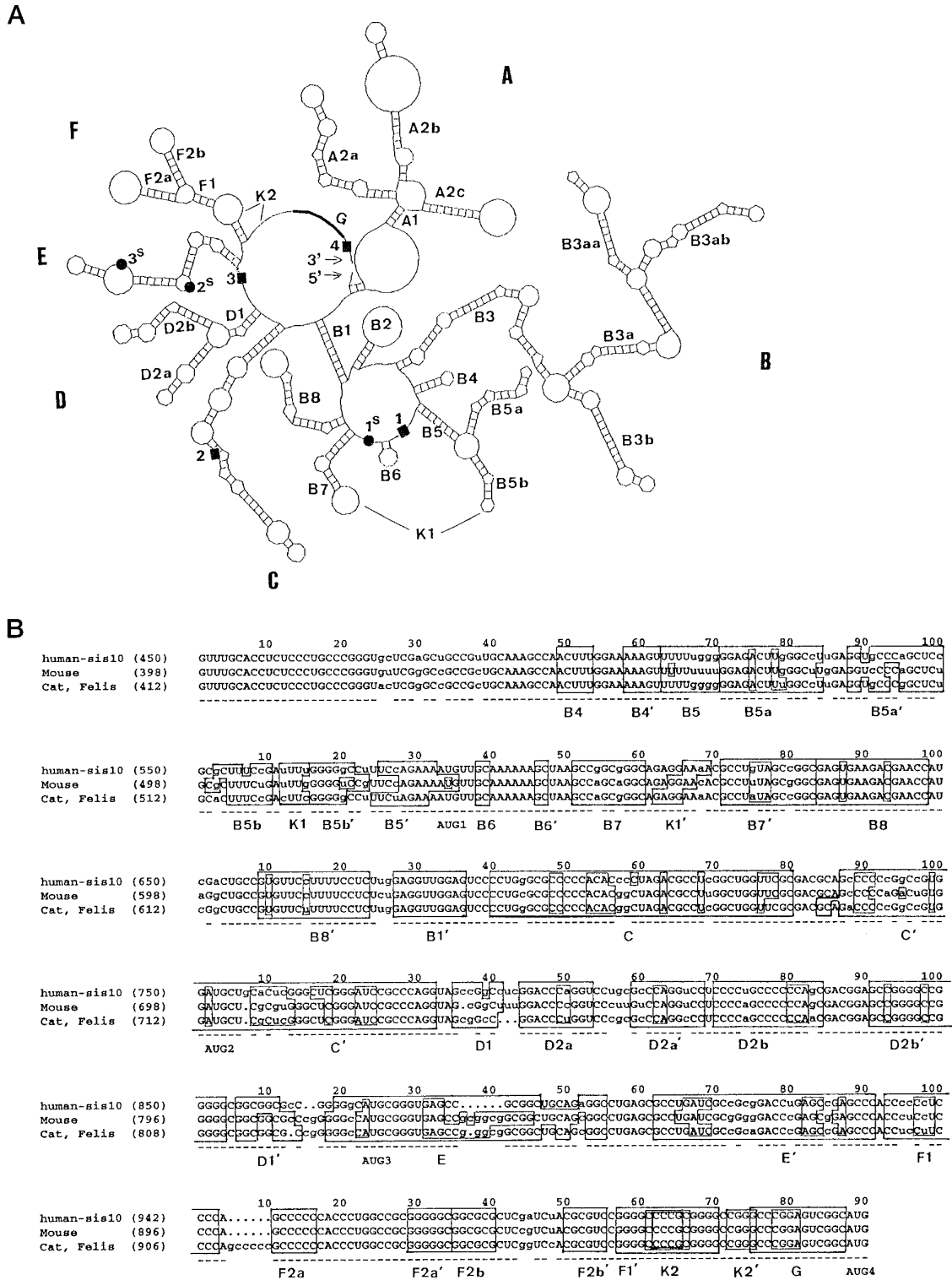


**FIG. 2. Secondary structure model of the 5'-UTR of human PDGF2.** A, conserved structure of PDGF2/*c-sis* 5'-UTR, which is composed of six domains, A–F. All stem-loop structures are marked and refer to specific nt regions of the 5'-UTR as follows: A, 4–187; A2a, 20–73; A2b, 74–128; A2c, 133–164; B, 192–685; B2, 202–226; B3, 231–495; B3a, 272–412; B3aa, 299–336; B3ab, 337–382; B3b, 413–455; B4, 498–511; B5, 512–581; B5a, 520–549; B5b, 552–570; B6, 587–596; B7, 600–632; B8, 633–672; C, 689–781; D, 784–860; D2a, 793–817; D2b, 819–853; E, 866–932; F, 934–1005; F2a, 946–969; F2b, 970–990. Nucleotide numbering refers to the human PDGF2/*c-sis* 5'-UTR (GenBank™ accession number M19719). RNA pseudoknot interactions are denoted by *K1* and *K2*. The three upstream AUG codons are denoted by *dark squares 1–3*, and the corresponding in-frame stop codons are denoted by *dark circles 1<sup>s</sup>–3<sup>s</sup>*. AUG4, the translational initiator codon, is positioned at nt 1023–1025 and denoted by *dark square 4*. Sequence homologous to 18 S rRNA is marked as a *heavier line* and denoted by the letter *G*. B, sequence alignment of the 3' portion of PDGF2/*c-sis* 5'-UTR. Sequences of human, mouse, and cat (GenBank™ accession numbers M19719, M64844, X05112, respectively) are shown. *Dots* indicate deletions. Conserved and nonconserved nt in the alignment are indicated by *upper* and *lowercase letters*, respectively. Conserved base pairing illustrated in A are marked by *boxes* and labeled by the letters B–B', C–C', D–D', E–E', F–F'. A nt in a *box* enclosed by another *box* failed to form an appropriate base pair. Positions of AUG codons are indicated. *Box G* shows the complementary sequence (5'-GCCcgaGUCGGC-3') to the 3'-end sequence (5'-GUCCGuaACaaGGU-3', nt 1826–1838) of human 18 S rRNA. Pseudoknot interactions are denoted by *K1* and *K2*.

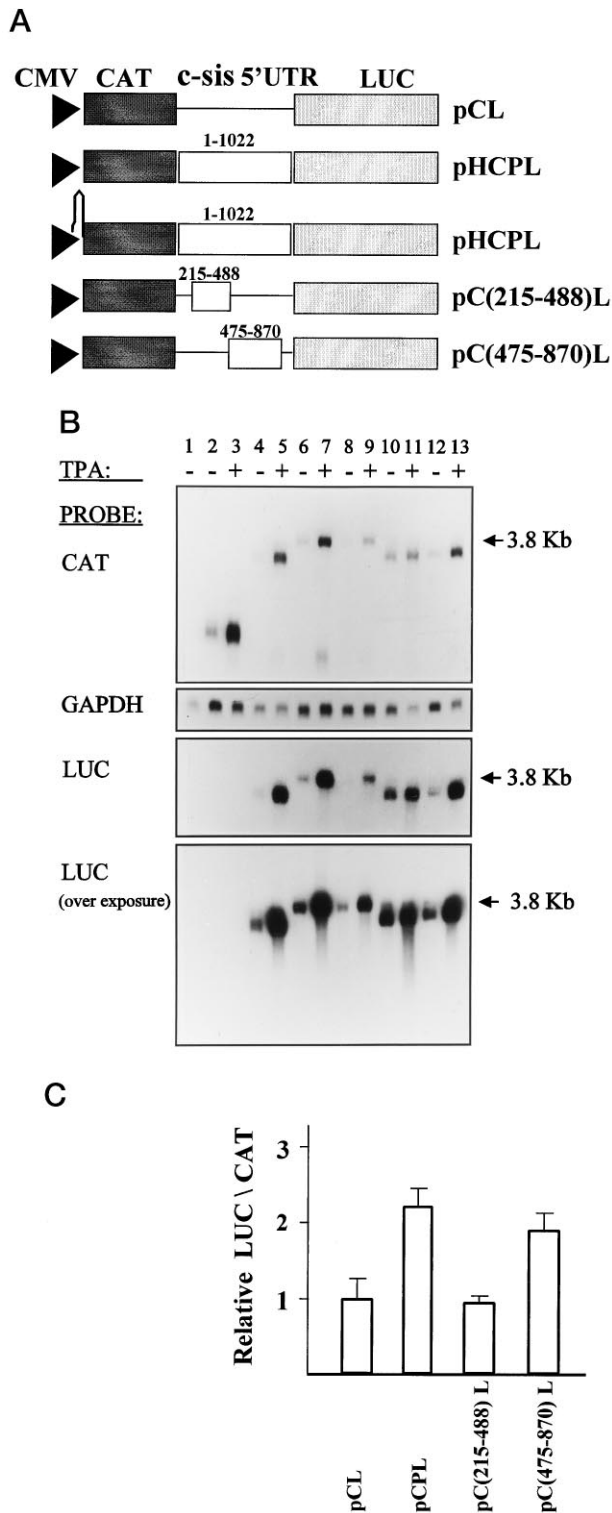


**FIG. 3. Effect of differentiation on *c-sis* IRES activity.** A, schematic drawing of the transcription unit of pCL, pHCL, pCPL, pC(215-488)L, and pC(475-870)L plasmids. pHCL contains a hairpin with stability of  $\Delta G = -40$  kcal mol<sup>-1</sup> upstream to CAT (see "Experimental Procedures"). Triangles, CMV promoter; dark boxes, the CAT coding sequence; open boxes, intact or truncated 5'UTR of *c-sis*, as indicated; light boxes, the LUC coding sequence. B, Northern blot analysis. K562 cells were mock-transfected (lane 1) or transfected with pCMV-CAT (lanes 2 and 3), pCL (lanes 4 and 5), pCPL (lanes 6 and 7), pHCL (lanes 8 and 9), pC(215-488)L (lanes 10 and 11), or pC(475-870)L (lanes 12 and 13), followed by incubation in medium with or without TPA (see "Experimental Procedures"). 72 h after the electroporation, poly(A)<sup>+</sup> RNA from 150  $\mu$ g of total RNA were used for Northern hybridization analysis using sequentially <sup>32</sup>P-labeled cDNA probes specific for CAT, LUC, or GAPDH, as indicated. Following each hybridization, the blot

led to elevation in the steady-state level of all the CMV promoter-driven mRNAs. However, in view of the integrity of the bi-cistronic mRNA molecules, both CAT and LUC proteins are believed to be translated from an intact bi-cistronic mRNA. Thus, the LUC/CAT ratio deduced from LUC and CAT enzymatic activities in the different samples reflects the relative translation efficiencies of both cistrons, regardless of the absolute mRNA level in the samples.

Fig. 3C shows the LUC/CAT ratio obtained in the differentiated cells relative to control cells for each of the plasmids. The pCL-derived LUC activity, which represents second cistron translation from an IRES-less mRNA, probably reflects some level of read-through, leaky scanning, re-initiation, or translation of undetectable degradation products of the bi-cistronic mRNA. However, such pCL-derived second cistron translation was hardly affected by TPA treatment (Fig. 3C, pCL). Insertion of region spanning nucleotides 215-488, which harbor structure B3 of the 5'-UTR (Fig. 2A) upstream of LUC, decreased LUC translation level about 2-fold compared with pCL (not shown), but did not change the relative LUC/CAT upon differentiation (Fig. 3C, pC(215-488)L). Insertion of the full-length (1022 nt) or a 395-nt segment spanning nucleotides 475-870, which harbor structures B4-D of the 5'-UTR (Fig. 2A), also decreased the second cistron translation by 5- or 2-fold, respectively, compared with pCL (not shown). However, these two segments were able to confer differentiation-linked LUC translation enhancement (Fig. 3C, pCPL and pC(475-870)L). In summary, the LUC/CAT ratio was not affected by the TPA treatment unless the full-length or a specific region of the 5'-UTR was inserted between the cistrons. These specific segments conferred about 2-fold enhancement in translation efficiency of the second cistron over the first cistron due to the TPA treatment. These observations suggest the presence of a differentiation-linked internal ribosomal binding site within the 5'-UTR of PDGF2/*c-sis*.

**The Effect of 5' Hairpin on Translation Efficiency**—To verify the ability of the 5'-UTR to confer internal translation, we tested its ability to confer 5'-end-independent translation to the second cistron. For that purpose, a hairpin structure with stability of  $\Delta G = -40$  kcal mol<sup>-1</sup> was inserted upstream of the first cistron of pCPL to create plasmid pHCL (Fig. 3A). Both pCPL and pHCL plasmids contain the entire PDGF2/*c-sis* 5'-UTR between the CAT and LUC cistrons. K562 cells were transfected with each of the plasmids, followed by 48-h incubation in control or TPA containing medium prior to detection of CAT and LUC enzymatic activities. The CAT or LUC expression levels obtained from the 5' hairpin-containing plasmid pHCL were compared with those from plasmid pCPL which lacks the 5' hairpin. As shown in Fig. 4A, translation of the first cistron represented by CAT activity was inhibited about 10-fold, whereas the second cistron translation represented by LUC activity was inhibited only about 3-fold by the 5' hairpin.

The lower CAT and LUC levels obtained from pHCL plasmid compared with pCPL might result in part from lower transfection efficiencies of pHCL. However, variation in transfection efficiencies cannot account for the difference between the relative expression of the two reporter genes. The relative CAT expression was always 3-fold lower than the rel-

was exposed for 15 h, except for the LUC blot, which was also subjected to longer exposure for 4 days to rule out the presence of shorter luciferase transcripts. C, K562 cells were transfected with each of the indicated plasmids as detailed in B. 72 h after the electroporation, CAT and LUC enzymatic activities were determined. The data represent the LUC/CAT ratio obtained in the TPA-treated cells relative to control cells. The bars represent the average  $\pm$  S.E. of three independent transfection experiments.

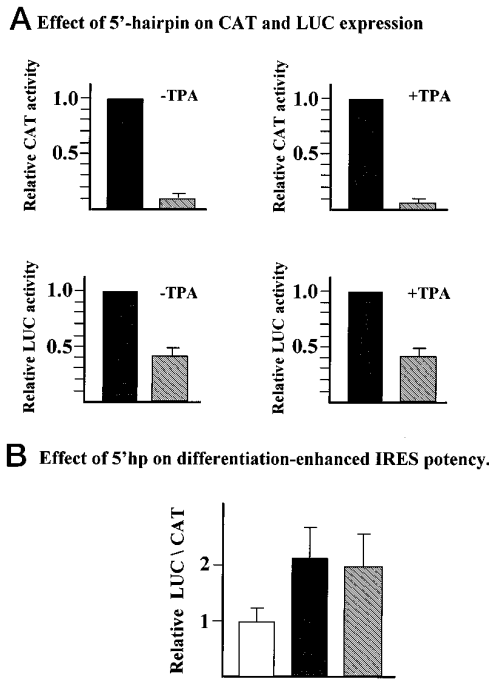


FIG. 4. **Effect of 5' hairpin.** K562 cells were transfected with pCPL (open bar), pCPL (dark bars), or pHCPL (striped bars) which are shown in Fig. 3A, followed by incubation in medium with (+TPA) or without TPA (-TPA). 72 h after electroporation, CAT and LUC enzymatic activities were determined. A, the pHCPL-derived LUC and CAT activities were compared with the pCPL-derived CAT or LUC activities, which were arbitrarily set as 1. The bars represent the average  $\pm$  S.E. of three independent transfection experiments. B, the data represent the LUC/CAT ratio obtained in the TPA-treated cells relative to control cells for each of the plasmids, as indicated.

ative LUC expression (Fig. 4A). Thus, the 5' hairpin inhibitory effect on the first cistron was 3–4-fold stronger than on the second cistron. This absolute dissimilarity of the 5' hairpin effect on translation of the two cistrons points to the ability of PDGF2/*c-sis* 5'-UTR to confer 5'-end-independent translation to the second cistron. As shown in Fig. 4A, PDGF2/*c-sis* conferred the 5'-end-independent translation in both the control (-TPA) as well as in the differentiated (+TPA) K562 cells. This observation indicates that the 5'-UTR harbors an IRES element that is active in both cellular conditions. However, the IRES potency varies with changes in the cellular milieu, as shown in Fig. 4B illustrating the LUC/CAT ratio in the differentiated cells relative to the control cells for each of the plasmids. The relative LUC/CAT ratio of the IRES-less plasmid was hardly changed by TPA treatment, while the effectiveness of the IRES was enhanced about 2-fold by the TPA treatment regardless of the 5'-end, as demonstrated for both pCPL and pHCPL. This experiment further signifies the differentiation-linked IRES activity of PDGF2/*c-sis* 5'-UTR.

#### DISCUSSION

Structural elements that determine the efficiency of translation initiation include the 5'-m<sup>7</sup>G cap structure, the context surrounding the initiator codon, 5'-UTR length, stability of secondary structures in the 5'-UTR, and presence or absence of open reading frames upstream of the initiator codon (uORFs) (1). A hairpin structure with predicted stability of  $\Delta G = -50$  kcal mol<sup>-1</sup> in the 5'-UTR was found to significantly inhibit protein synthesis (26). In addition, uORFs, which in some cases have a regulatory role (27), were found to decrease the frequency of initiation of the major ORF. Thus, it is not surprising that the extraordinarily long PDGF2/*c-sis* 5'-UTR, which contains stable secondary structures and three uORFs acts as a

strong translational inhibitor (4–6, 28). Mutations of the uORFs did not relieve the inhibitory effect (5–6, 28). This observation, together with the highly stable secondary structures ( $\Delta G = -270$  kcal mol<sup>-1</sup>) within the PDGF2/*c-sis* 5'-UTR, raised a question about the ability of ribosomes to linearly scan along this mRNA leader from its 5'-end according to the conventional scanning model (29).

As demonstrated in this study, when the PDGF2/*c-sis* 5'-UTR was placed upstream of the second cistron in a bi-cistronic vector, it conferred a differentiation-linked enhancement of translation with preference for the second cistron (Figs. 3C and 4B). However, regardless of the cellular conditions, the 5' hairpin inhibitory effect on the first cistron was 3–4-fold stronger than on the second cistron, indicating the inherent ability of PDGF2/*c-sis* 5'-UTR to confer internal translation to the second cistron even before differentiation (Fig. 4A). These observations indicate the presence of an IRES element within PDGF2/*c-sis* 5'-UTR which has low or high activity depending on the cellular milieu. As shown in Figs. 1B, 3C, and 4B, the PDGF2/*c-sis* IRES potency was enhanced about 2-fold by TPA treatment. These data do not match our previous experiments with monocistronic vectors showing 8-fold 5'-UTR-mediated translational enhancement upon TPA treatment (4). We strongly believe that the stronger effect observed using monocistronic vectors reflects the behavior of the authentic PDGF2/*c-sis* mRNA. Sequences flanking the 5'-UTR in the bi-cistronic vector may dramatically affect its folding and consequently its IRES activity. This discrepancy is analogous to the discrepancies reported previously for other IRES elements studied in the context of mono- and bi-cistronic vectors (11, 30–31). In addition, since luciferase protein is very unstable compared with CAT (32), LUC activity reflects the level of newly synthesized LUC molecules, whereas CAT activity represents the total accumulated CAT enzyme. Thus, the relative LUC/CAT ratio, which in this study was used to measure IRES potency, can detect only the differentiation-linked enhancement phenomenon and not its actual intensity.

The evolutionary conservation of the stable secondary structures predicted for the PDGF2/*c-sis* mRNA leader, and the conserved complementarity to 18 S rRNA immediately upstream of the major ORF (Fig. 2), strongly suggest a role in mediating internal translation. The D-IRES activity was conferred by the full-length (1022 nt) 5'-UTR or by a 395 nt segment spanning nucleotides 475–870 of the 5'-UTR. In contrast, the 273-nt segment spanning nucleotides 215–488 of the 5'-UTR did not confer D-IRES activity and thereby served as a negative control in our experiments (Fig. 3). Interestingly, this non-IRES segment, harboring structure B3 (Fig. 2A), is composed of highly stable stem-loop structures and is located upstream of the D-IRES-conferring segment. Hence, we suggest that the role of structure B3 is to inhibit PDGF2/*c-sis* mRNA translation in case it is present at the wrong tissue or time, by imposing a barrier to ribosomal scanning. As shown previously, the 5'-UTR-mediated translation inhibition is relieved during megakaryocytic differentiation of K562 cells (4). The present study demonstrates that translational inhibition relief is achieved by enhanced activity of an IRES element that resides downstream of structure B3, the scanning barrier.

It can be argued that expression of the major ORF reflects translation of undetectable shorter transcripts that are transcribed from a cryptic promoter and therefore lack most of the inhibitory 5'-UTR. Our data rule out this possibility for PDGF2/*c-sis*, since we used both cytoplasmic and nuclear expression systems. The cytoplasmic system employed the bacteriophage T7 promoter in the cytoplasm of vaccinia virus-infected cells, in which the host protein synthesis is shut off by

the virus. The fact that the D-IRES phenomenon was observed in that cytoplasmic expression system (Fig. 1B) proves that a cryptic promoter activity within the PDGF2/*c-sis* 5'-UTR is not responsible for the differentiation-linked enhanced expression effect. We cannot rule out possible translation of degradation products that contain only the second cistron, but such a phenomenon does not negate our interpretation, since the small amount of potential degradation products is probably similar in all the samples, including the control plasmid pCL (Fig. 3B).

It has become clear that a given cell type can qualitatively and quantitatively affect the expression of the PDGF A and B chains at the levels of transcription, RNA processing, translation, and post-translation modifications (3). The presence of an IRES element within PDGF2/*c-sis* 5'-UTR defines a functional role to the cumbersome mRNA leader and justifies its conserved unusual architecture. The evolutionary conservation of the secondary structures hints that the IRES activity is mediated by evolutionary conserved RNA-binding proteins. We speculate that the availability of such *trans*-acting factors differs in response to specific signals according to the cell's need. The differentiation-linked enhancement of PDGF2/*c-sis* IRES activity might involve post-translational modifications of existing proteins or synthesis of new proteins with RNA binding activity. Apparently, the profile of proteins that bind to PDGF2/*c-sis* 5'-UTR dramatically changes due to differentiation of K562 cells.<sup>2</sup> It has become evident that viral IRES elements require cellular *trans*-acting RNA binding proteins for their function (reviewed in Ref. 7). Thus, some of the differentiation-induced *trans*-acting factors might also mediate the IRES activity of certain viruses. The enhanced IRES activity of EMCV in the TPA-treated K562 cells (Fig. 1) supports this notion and underscores the importance of cell type to virulence potential. In addition, the variable potency of different known IRES elements might result from variable binding affinities to common factors and/or different requirements for additional tissue-specific factors. In contrast to viral IRES elements, cellular IRES elements are expected to be much less potent. Indeed, we found that PDGF2/*c-sis* IRES is about 10-fold less active in TPA-treated K562 cells than EMCV IRES (not shown).

PDGF belongs to a subclass of genes that encode for regulatory proteins with a major role in cell proliferation. Among these are several proto-oncogenes as well as growth factors, cytokines, receptors, and transcription factors (2). A typical property of these genes is their tight expression regulation to guarantee correct protein level at the appropriate time and location. An associated feature is their complex architecture, that is, *cis*-regulatory elements that mediate expression level in response to signals. The stringent regulation is a result of various mechanisms that simultaneously control expression at multiple levels. One of the *cis*-elements shared by the above subclass of genes is their extraordinarily long, structured and AUG-burdened mRNA leader, which provides a built-in blockade against efficient ribosomal scanning. Although leaky scanning and reinitiation are the mechanisms responsible for some translation modulation phenomena (reviewed in Ref. 27), a conditional internal ribosomal entry may also provide a widespread mechanism for translation regulation. First, it gives certain mRNA molecules cap-independent translation ability in response to viral infection or stress conditions, as was shown for immunoglobulin heavy-chain binding protein (BiP) IRES (9) and recently proposed for eIF4G IRES (12). Second, it can enforce an alternative translational start site, resulting in translation of different proteins from the same mRNA mole-

cule, as mediated by the IRES element of FGF2 (10). Third, it may provide a developmentally regulated protein synthesis like that proposed for the homeotic gene *Antennapedia* of *D. melanogaster* and for human IFG-II leader 1 IRES elements (13, 11). The present study provides evidence for a differentiation-linked IRES element residing within a cumbersome mRNA leader. In the absence of appropriate *trans*-acting factors, it may provide a double safety control mechanism, since it prevents efficient translation of the mRNA in cases of uncontrolled transcription. Upon differentiation, the IRES becomes more active, leading to efficient protein synthesis. The translational enhancement has an additive effect with other levels of control to achieve significant expression enhancement in the appropriate time window during differentiation. This mechanism, which provides an additional step to the fine tuning of PDGF2/*c-sis* gene expression, might be employed by numerous critical regulatory genes with unusual 5'-UTRs and might have widespread implications for cellular growth and development.

**Acknowledgments**—We thank P. Sarnow for pT7CAT-LUC plasmid and A. C. Prats for pBI-FC1 and pHP-FC1 plasmids. We also thank E. Guetta, Z. Stein, and G. Rotman for helpful comments.

**Addendum**—After completion of the study, we have noticed that TPA from Calbiochem is more potent than that of Sigma with regards to the effects measured in this research.

#### REFERENCES

- Merrick, W. C., and Hershey, J. W. B. (1996) *Translational Control* (Hershey, J. W. B., Mathews, M. B., and Sonenberg, N., eds) pp. 31–69, Cold Spring Harbor Laboratory Press, NY
- Kozak, M. (1991) *J. Cell Biol.* **115**, 887–903
- Dirks, R. H., and Bloemers, H. P. J. (1996) *Mol. Biol. Rep.* **22**, 1–24
- Bernstein, J., Shefler, I., and Elroy-Stein, O. (1995) *J. Biol. Chem.* **270**, 10559–10565
- Rao, C. D., Pech, M., Robbins, K. C., and Aaronson, S. A. (1988) *Mol. Cell. Biol.* **8**, 284–292
- Horvath, P., Saganuma, A., Inaba, M., Pan, Y.-B., and Gupta, K. (1995) *Cell Growth & Diff.* **6**, 1103–1110
- Jackson, R. J., and Kaminski, A. (1995) *RNA (N.Y.)* **1**, 985–1000
- Rivera, V. M., Welsh, J. D., and Maizel, J. V. (1988) *Virology* **165**, 42–50
- Macejak, D. G., and Sarnow, P. (1991) *Nature* **353**, 90–94
- Vagner, S., Gensac, M.-C., Maret, A., Bayard, F., Amalric, F., Prats, H., and Prats, A.-C. (1995) *Mol. Cell. Biol.* **15**, 35–44
- Teerink, H., Voorma, H. O., and Thomas, A. A. M. (1995) *Biochim. Biophys. Acta* **1264**, 403–408
- Gan, W., and Rhoads, R. E. (1996) *J. Biol. Chem.* **271**, 623–626
- Oh, S.-K., Scott, M. P., and Sarnow, P. (1992) *Genes Dev.* **6**, 1643–1653
- Whetter, L. E., Day, S. P., Elroy-Stein, O., Brown, E. A., and Lemon, S. M. (1994) *J. Virol.* **68**, 5253–5263
- Cohen, J. I., Ticehurst, J. R., Feinstone, S. M., Rosenblum, B., and Purcell, R. H. (1987) *J. Virol.* **61**, 3035–3039
- Bradford, M. M. (1976) *Anal. Biochem.* **72**, 248–254
- Sambrook, J., Fritsch, E. F., and Maniatis, T. (1989) *Molecular Cloning: A Laboratory Manual*, Cold Spring Harbor Laboratory, Cold Spring Harbor, NY
- Ehrenfeld, E. (1996) *Translational Control* (Hershey, J. W. B., Mathews, M. B., and Sonenberg, N., eds) pp. 549–573, Cold Spring Harbor Laboratory Press, NY
- Le, S.-Y., Chen, J.-H., and Maizel, J. V., Jr. (1993) *Nucleic Acids Res.* **21**, 2173–2178
- Le, S.-Y., and Maizel, J. V., Jr. (1989) *J. Theor. Biol.* **138**, 495–510
- Le, S.-Y., Chen, J.-H., and Maizel, J. V., Jr. (1990) *Structure and Methods: Human Genome Initiative and DNA Recombination* (Sarma, R. H., and Sarma, M. H., eds) Vol. 1, pp. 127–136, Adenine Press, New York
- Pilipenko, E. V., Gmyl, A. P., Maslova, S. V., Svitkin, Y. V., Sinyakov, A. N., and Agol, V. I. (1992) *Cell* **68**, 119–131
- Le, S.-Y., Chen, J.-H., Sonenberg, N., and Maizel, J. V., Jr. (1993) *Nucleic Acids Res.* **21**, 2445–2451
- Scheper, G. C., Voorma, H. O., and Thomas, A. A. M. (1994) *FEBS Lett.* **352**, 271–275
- Le, S.-Y., Siddiqui, A., and Maizel, J. V., Jr. (1996) *Virus Genes* **12**, 135–147
- Pelletier, J., and Sonenberg, N. (1985) *Cell* **40**, 515–526
- Geballe, A. P. (1996) *Translational Control* (Hershey, J. W. B., Mathews, M. B., and Sonenberg, N., eds) pp. 173–197, Cold Spring Harbor Laboratory Press, NY
- Ratner, L. (1989) *Nucleic Acids Res.* **17**, 4101–4115
- Kozak, M. (1989) *J. Cell Biol.* **108**, 229–241
- Van der Velden, A., Kaminski, A., Jackson, R., and Belsham, G. J. (1995) *Virology* **214**, 82–90
- Witherell, G. W., Schultz-Witherell, C. S., and Wimmer, E. (1995) *Virology* **214**, 660–663
- Gould, S. J., Keller, G.-A., Hosken, N., Wilkinson, J., and Subramani, S. (1989) *J. Cell Biol.* **108**, 1657–1664

<sup>2</sup> O. Sella, J. Bernstein, and O. Elroy-Stein, manuscript in preparation.